

See discussions, stats, and author profiles for this publication at: <https://www.researchgate.net/publication/6251212>

# The Influence of Sodium Perfluorooctanoate on the Conformational Transitions of Human Immunoglobulin

ARTICLE *in* THE JOURNAL OF PHYSICAL CHEMISTRY B · JULY 2007

Impact Factor: 3.3 · DOI: 10.1021/jp071394k · Source: PubMed

CITATIONS

4

READS

24

8 AUTHORS, INCLUDING:



**Paula V Messina**

Universidad Nacional del Sur

75 PUBLICATIONS 634 CITATIONS

SEE PROFILE



**Xerardo Prieto**

University of Santiago de Compostela

111 PUBLICATIONS 1,677 CITATIONS

SEE PROFILE



**Veronica I Dodero**

Bielefeld University

26 PUBLICATIONS 174 CITATIONS

SEE PROFILE



**Juan M. Ruso**

University of Santiago de Compostela

163 PUBLICATIONS 2,042 CITATIONS

SEE PROFILE

# The Influence of Sodium Perfluorooctanoate on the Conformational Transitions of Human Immunoglobulin

Paula V. Messina,<sup>\*,#</sup> Gerardo Prieto,<sup>†</sup> Francisco Salgado,<sup>§</sup> Carla Varela,<sup>§</sup> Montserrat Nogueira,<sup>§</sup> Verónica Dodero,<sup>‡</sup> Juan M. Ruso,<sup>†</sup> and Félix Sarmiento<sup>\*,†</sup>

*Biophysics and Interfaces Group, Department of Applied Physics, Faculty of Physics, University of Santiago de Compostela, 15782 Santiago de Compostela, Spain, Department of Biochemistry and Molecular Biology, Faculty of Biology, University of Santiago de Compostela, 15782, Santiago de Compostela, Spain, and Department of Organic Chemistry, Faculty of Chemistry, University of Santiago de Compostela, 15782 Santiago de Compostela, Spain*

*Received: February 19, 2007; In Final Form: May 10, 2007*

In the field of bioscience, the study of the interactions between blood proteins and fluorinated materials is very important from both theoretical and applied points of view. Fluorinated materials have potential use in drug delivery, as blood substitutes, and in biotechnology. Using a combination of ultraviolet–visible (UV–vis) and ultraviolet–circular dichroism (UV–CD) spectroscopies and ion-selective electrodes, the complete interaction of sodium perfluorooctanoate (SPFO) and the most important immunoglobulin (on a quantitative basis) in human serum, immunoglobulin G (IgG), has been evaluated. The study has been focused on bulk solution. By the application of an SPFO selective electrode, it was determined that there were true specific unions between surfactant molecules and IgG structure. The experimental data were presented as Koltz and Scatchard plots and analyzed on the basis of an empirical Hill equation. The conformational changes at the bulk solution were well characterized by UV–vis and UV–CD spectroscopies. As a consequence of these changes, the protein structure was affected.

## 1. Introduction

Fluorinated amphiphiles constitute novel and versatile components useful for preparing films and membranes, elaborating and stabilizing colloidal systems, coating and dispersing micro- and nanoparticles, protecting large bioengineered molecules, and modulating the response of temperature and pH-sensitive materials.<sup>1</sup> The self-association of fluorosurfactants in discrete objects, such as vesicles and tubules, occurs with molecules that are often structurally simpler (shorter, single-tailed, non-chiral, and non-hydrogenated-bonding) than those in the hydrocarbon series. This should facilitate the finding of relationships among structured properties and the elucidation and understanding of the role of individual contributors to a given association phenomenon. In contrast to fluorocarbons, the pharmacology of fluorinated amphiphiles is still in its infancy. Adsorption, distribution, metabolism, and excretion studies are badly needed. The results of these studies will largely determine the extent to which fluorosurfactants may be used in pharmaceuticals.<sup>2</sup> In this sense, it is important to study the interaction between perfluorinated surfactants and blood proteins.

In previous works,<sup>3–5</sup> we have studied the interaction of the fluoroamphiphile sodium perfluorooctanoate (SPFO) and the protein human serum albumin (HSA). From these studies, it was established that the interaction between the components have a pronounced effect on the physicochemical properties of

the above system, as well as on the structure of formed adducts and complexes. Our results suggest that, at dilute surfactant solutions, protein molecules tend to locate themselves at the aqueous–air interface as well as SPFO molecules. Under these conditions, protein and surfactant concentrations in the bulk solution were negligible, and interaction occurred only at interfaces. The SPFO induced conformational changes on the HSA structure at the air–aqueous interface. On the contrary, at concentrated solutions, it is possible to appreciate that the surfactant produces conformational changes in the protein conformation at the bulk solution, and this fact affects the latter protein adsorption.

In this work we extended our studies to evaluate the complete interaction of SPFO and the second major soluble protein constituent of the circulatory system, immunoglobulin G (IgG). The antibodies or immunoglobulins were the first to be identified as serum molecules capable of neutralizing a number of infectious organisms. It was the availability of large amounts of immunoglobulins (in human serum, the concentration of IgG is about 13.5 g/L) that led to early elucidation of their primary and tertiary structure. IgG (molecular mass, 150 000 Da) is a Y-shaped tetrameric glycoprotein formed from a series of globular domains. It consists of two light chains and two identical heavy chains, cross-linked by interchain disulfide bonds and stabilized by noncovalent interactions. Light chains are folded into two globular domains, while heavy chains comprise five domains. Its structural motif is composed of two-stacked- $\beta$ -plated sheets surrounding an interior packed with hydrophobic residues. It has domains with high specificity to bind analytes, whereas other domains of IgG promote protein unfolding to a surface in the proper orientation.

\* To whom correspondence should be addressed. Tel.: +34 981-563-100, ext. 14045. Fax: +34 981-520-676. E-mail: fsarmi@usc.es.

<sup>†</sup> Faculty of Physics.

<sup>§</sup> Faculty of Biology.

<sup>‡</sup> Faculty of Chemistry.

<sup>#</sup> Present address: Department of Chemistry, National University of Sud, Bahía Blanca, Argentine.

The aim of this study is to characterize the interaction between IgG and SPFO in order to obtain information on the effect of fluorinated surfactants in their interaction with blood proteins. As physical techniques, a combination of ultraviolet–visible (UV–vis) and ultraviolet–circular dichroism (UV–CD) spectroscopies and ion-selective electrodes have been used.

## 2. Experimental Section

**2.1. Materials.** SPFO ( $C_7F_{15}COO^-Na^+$ ; analytical grade, 97%, product no. 16988) was from Lancaster MTM Research Chemicals, Ltd.

**2.2. IgG Purification.** Human serum was collected from healthy donors and stored at  $-20\text{ }^{\circ}\text{C}$  until used. Samples of 1 mL were thawed and centrifuged at  $4\text{ }^{\circ}\text{C}$  for 15 min at 13 000g, and the supernatant was gently mixed with 37 mg of potassium sulfate with soft shaking. After centrifugation at 13 000g for 15 min, the supernatant was carefully collected and filtered by using a  $0.22\text{ }\mu\text{m}$  filter (Amicon). To select the IgG, a T-Gell adsorbent column (Pierce) was used according to the manufacturer's instructions with modifications in order to optimize the quantitative and qualitative yield. Briefly, the sample, 1 mL of serum with a final concentration of 0.5 M potassium sulfate, was loaded in a T-Gell column previously equilibrated with binding buffer (Pierce) at room temperature. After being washed with 15 mL of binding buffer, immunoglobulins were eluted with 10 mL of elution buffer, and fractions of 3 mL were collected. The elution of IgG was monitored at 280 nm, with the greater absorbance corresponding to the fraction 2. The amount of protein bound to the matrix was determined by a BCA test according to the manufacturer's instructions. Routinely, 12% of the total protein from the serum sample was bound to the matrix, which represents 90% of the standardized amount of immunoglobulins present in human healthy blood. To set both the qualitative and quantitative IgG yield, fraction 2 and the no-bound material were analyzed by two-dimensional electrophoresis and silver staining. Gels from both samples showed that (1) only immunoglobulins were retained in the column matrix, and (2) no immunoglobulins were visualized in the gel corresponding to the nonbound material. Purified IgG was dialyzed against MilliQ water and aliquots of 1 mg/mL stored at  $-20\text{ }^{\circ}\text{C}$ .

**2.3. Preparation of Solutions.** SPFO stock solution (1 mg/mL) was prepared by directly dissolving the appropriate amount of surfactant in MilliQ water. IgG stock solution (1 mg/mL) was obtained from the previously described synthesis method. Both solutions were kept in a refrigerator before use ( $-20\text{ }^{\circ}\text{C}$ ) and diluted as required. IgG solutions were prepared without buffer addition, given that its presence could affect surface tension measurements.

**2.4. Absorbance Measurements.** Difference spectra were measured with a Beckman spectrophotometer (model DU 640) with six microcuvettes, which operates in UV–vis region (from 190 to 1100 nm) of the electromagnetic spectrum wavelength. All measurements were made using IgG–SPFO mixed solutions containing a fixed IgG concentration ( $0.015\text{ mg/mL} = 0.1\text{ }\mu\text{M}$ ) and SPFO in the concentration range of 0.001–30 mM, in a pair of carefully matched quartz cuvettes ( $1\text{ cm}^3$  capacity) in the wavelength range of 240–310 nm. Measurements were taken from freshly prepared solutions due to the fast degradation of IgG. At least four measurements of difference spectra were made.

**2.5. Potentiometry, Ion-Selective Electrode.** Potentiometric determinations were made with a millivoltmeter and a CRISON pH meter. The millivoltmeter was used with a  $C_7F_{15}COO^-$

ion-selective electrode, against a saturated calomel electrode. The  $C_7F_{15}COO^-$  electrode was made by gluing a membrane (made with 300 mg of poly(vinyl chloride) (PVC) dissolved in 50 mL of tetrahydrofuran (THF) and 0.2 mL of dibutylphthalate (plasticizer) and 0.167 g of  $Ba^{2+}(C_7F_{15}COO^-)_2$ ) to one end of a PVC tube. This salt was made by mixing the appropriate amounts of  $Ba(OH)_2$  and  $C_7F_{15}COO^-Na^+$  aqueous solution. The insoluble  $Ba^{2+}(C_7F_{15}COO^-)_2$  salt was filtered and washed several times with double-distilled water and then left to dry. The crystals were powdered and suspended in the PVC solution. Then, the suspension was left in a Petri dish to let the THF evaporate, and the resulting membrane was cut and glued to the tube. The tube was filled with an aqueous solution of  $0.01\text{ mol dm}^{-3}$   $C_7F_{15}COO^-Na^+$  and  $0.1\text{ mol dm}^{-3}$  KCl, which also contained a small amount of solid AgCl. An Ag/AgCl electrode made from a silver wire was placed into the tube and connected to the millivoltmeter by a copper wire passing through a rubber plug. The scheme of the electrode is Ag/AgCl/reference solution/PVC membrane/sample//AgCl/Ag. The time response of the electrode depends on  $C_7F_{15}COO^-Na^+$  concentrations, the added electrolyte, the stirring, and the conditioning. In dilute solutions, the time required to get stable electromotive force (emf) values was 10 min. Ion-selective electrodes are sensitive to the respective free (nonaggregated) ion activity. Because we worked with diluted solutions below the critical micelle concentration of  $C_7F_{15}COO^-Na^+$ , we assumed that all surfactants present in solution were free and that activities could approximate concentrations. The emf values obtained for the ion-selective electrode application to the  $C_7F_{15}COO^-Na^+$  aqueous solutions in the concentration range of 0.001–24 mM were plotted versus the logarithm of the total  $C_7F_{15}COO^-Na^+$  concentration. This calibration curve was employed to obtain the  $[C_7F_{15}COO^-]_{\text{free}}$  and  $\nu$  (the number of moles of ligand per mole of protein) values for the IgG–surfactant interaction. Protein concentration ( $0.1\text{ }\mu\text{M}$ ) remains constant during the whole experiment, and surfactant solution was added to vary its concentration from 0.001 to 24 mM.

**2.6. Circular Dichroism (CD) Measurements.** Far-UV–CD spectra were obtained using a JASCO-715 automatic recording spectropolarimeter (Japan) with a JASCO PTC-343 Peltier-type thermostated cell holder. Quartz cuvettes with a 0.2 cm path length were used. CD spectra of pure IgG and IgG– $C_7F_{15}COO^-Na^+$  dilute solutions were recorded from 195 to 380 nm. Protein concentration was  $1\text{ }\mu\text{M}$ , and surfactant concentrations varied from 0.10 to 50 mM. The following settings were used: resolution, 1 nm; bandwidth, 1 nm; sensitivity,  $50\text{ mdeg}$ ; response time, 8 s; accumulation, 3; and scan rate,  $50\text{ nm/min}$ . Corresponding absorbance contributions of buffer solution and water were subtracted with the same instrumental parameters. Data are reported as molar ellipticity and were determined as

$$[\theta]_{\lambda} = \frac{\theta_{\lambda} M_r}{ncl} \quad (1)$$

where  $c$  is the protein concentration,  $l$  is the path length of the cell,  $[\theta]_{\lambda}$  is the measured ellipticity at a wavelength  $\lambda$ ,  $M_r$  is the molecular mass of the protein, and  $n$  is the number of residues. Temperature denaturation was followed by the CD responses at 206 nm from 5 to  $80\text{ }^{\circ}\text{C}$ .

## 3. Results and Discussion

**3.1. Binding of SPFO to IgG.** The ability of a polypeptide chain to fold up into a unique and highly ordered structure is

the most important feature that differentiates a biologically active protein from an inert polymer. The interaction of ionic surfactants with globular proteins has been studied extensively.<sup>6,7</sup> It has been well-established that such interactions frequently lead to the destruction of the native structure of protein and the formation of unfolded protein–surfactant complexes. Due to the importance of denaturation studies that are capable of yielding information about the native state,<sup>8</sup> understanding the mechanism of surfactant binding is very important.

To interpret the binding data, the experimental results were analyzed using the Hunston<sup>9</sup> and Scatchard<sup>10</sup> plots. For this end, the concept of binding capacity ( $\Theta$ ) was used. It is the homotropic second derivative of the binding potential with respect to the chemical potential of the ligand ( $\mu_i$ ) and provides a measure of the steepness of the binding isotherm.<sup>11</sup> It represents the change in the number of moles of ligand per mole of macromolecule ( $\nu$ ) that accompanies a change in the chemical potential of that ligand.

By considering the ideal behavior  $\mu_i = \mu_i^0 + RT \ln[S]_{\text{free}}$ , binding capacity is equal to

$$\Theta = \left( \frac{\partial \nu}{\partial \mu_i} \right)_{T,P,\mu_j \neq i} = \left( \frac{1}{RT} \frac{\partial \nu}{\partial \ln[S]_{\text{free}}} \right)_{T,P,\mu_j \neq i} \quad (2)$$

where  $R$ ,  $T$ , and  $[S]_{\text{free}}$  are the gas constant, the absolute temperature, and the free concentration of the ligand, respectively. For such a system, the binding data can be analyzed on the basis of an empirical Hill equation:<sup>12</sup>

$$\nu = \frac{g(k_H[S]_{\text{free}})^{n_H}}{1 + (k_H[S]_{\text{free}})} \quad (3)$$

This can be written in the logarithmic form as follows:

$$\ln\left(\frac{\nu}{g - \nu}\right) = n_H + \ln k_H + n_H \ln[S]_{\text{free}} \quad (4)$$

where  $g$ ,  $k_H$  and  $n_H$  are the number of ligand-binding sites, the Hill binding constant, and the Hill coefficient, respectively.

Using eq 2, the binding capacity is equal to

$$\Theta = \frac{n_H \nu (g - \nu)}{gRT} \quad (5)$$

The Hill coefficient is defined as the slope of the Hill graph,

$$n_H = \frac{d \ln\left(\frac{y}{1-y}\right)}{d \ln[S]_{\text{free}}} = \frac{1}{y(1-y)} \frac{dy}{d \ln[S]_{\text{free}}} \quad (6)$$

where  $y$  is the fractional saturation of the macromolecule by the ligand, which is defined as

$$y = \frac{\nu}{g} \quad (7)$$

From the definition of binding capacity (eq 2), the following equations can be written:

$$n_H = \frac{RT\Theta}{gy(1-y)} \quad (8)$$

$$\Theta = \frac{n_H \nu (1-y)}{RT} \quad (9)$$

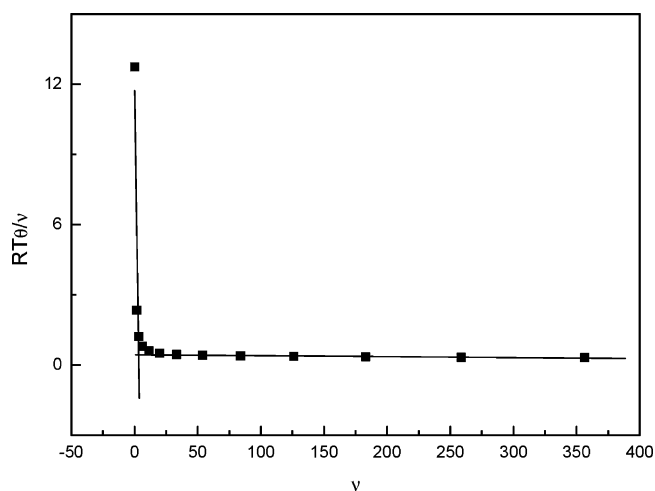


**Figure 1.** Variation of  $RT\Theta/\nu$  vs  $\nu$  plot for the interaction of SPFO with IgG at 25 °C.

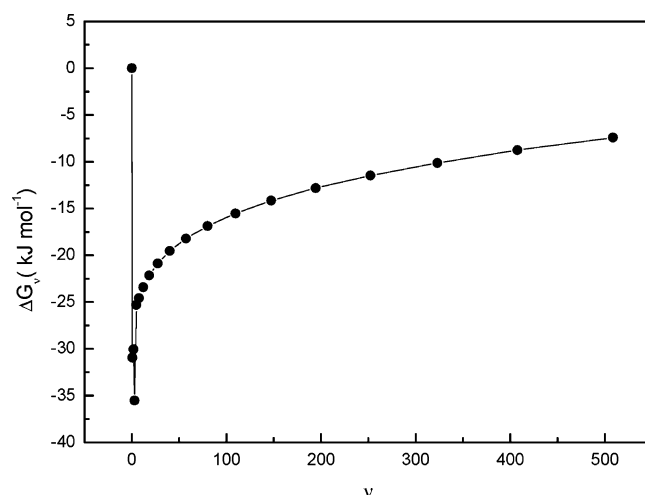


**Figure 2.** Gibbs energy of binding ( $\Delta G_\nu$ ) of SPFO to IgG as a function of surfactant ions bound ( $\nu$ ) at 25 °C.

Keeping in mind eq 7, eq 9 can be rearranged to the following manner:

$$\frac{RT\Theta}{\nu} = n_H - \frac{n_H \nu}{g} \quad (10)$$

This equation suggests that the plot of  $RT\Theta/\nu$  versus  $\nu$  for a system with “ $g$ ” identical and dependent binding sites should be linear. The slope and the ordinate and abscissa intercepts are equal to  $(-n_H/g)$ ,  $n_H$ , and  $g$ , respectively.

Binding data indicate that SPFO manifests a high affinity for IgG molecules with saturated values of 250 molecules of SPFO bound per IgG molecule.

The  $RT\Theta/\nu$  versus  $\nu$  plot for this system is shown in Figure 1. This curve can be divided in two linear regions. The values of the  $x$ -intercept of the first and second parts in the Figure 1 plot should be equal to  $g_1$  and  $g_1 + g_2$ , respectively. The values of  $n_{H1}$  and  $n_{H2}$  can be determined from the slope of the lines. Values of  $11.63 \pm 4.40$ ,  $0.43 \pm 0.01$ ,  $3 \pm 1$ , and  $1102 \pm 34$  were estimated for  $n_{H1}$ ,  $n_{H2}$ ,  $g_1$ , and  $g_2$ , respectively. This fact implies that, for SPFO–IgG interactions, all of the binding sites can be divided into two categories, each of them related to a binding set (named 1 and 2, respectively) with a relatively high difference in their binding affinity.

The obtained results seem to show that a strong ( $n_{H1} = 11.63$ ) ionic binding interaction between SPFO molecules to the IgG

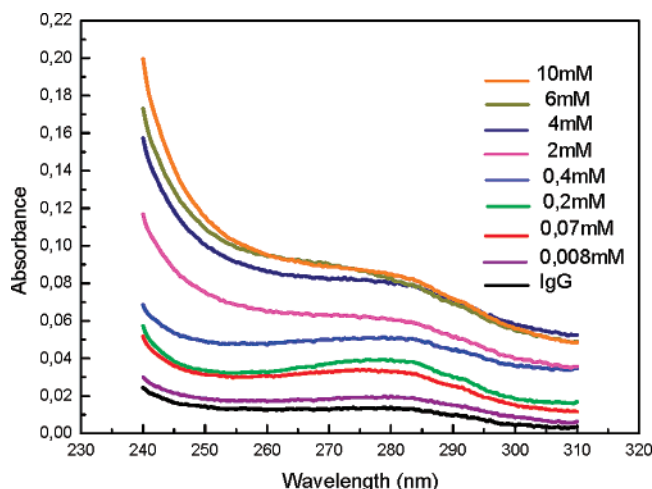


**Figure 3.** UV-vis spectra of the native protein (0.015 mg/mL) and IgG-SPFO mixtures for different SPFO concentrations.

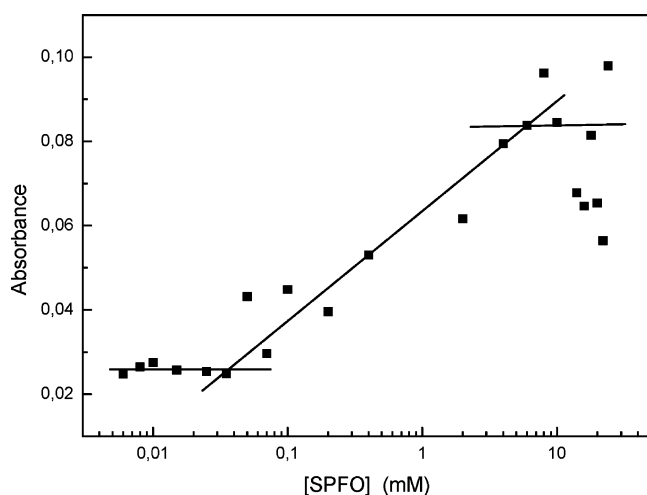


**Figure 4.** Absorbance variation of IgG at 280 nm vs [SPFO]. The IgG concentration was 0.0150 mg/mL (0.1  $\mu$ M). Estimated uncertainties are less than 2%.

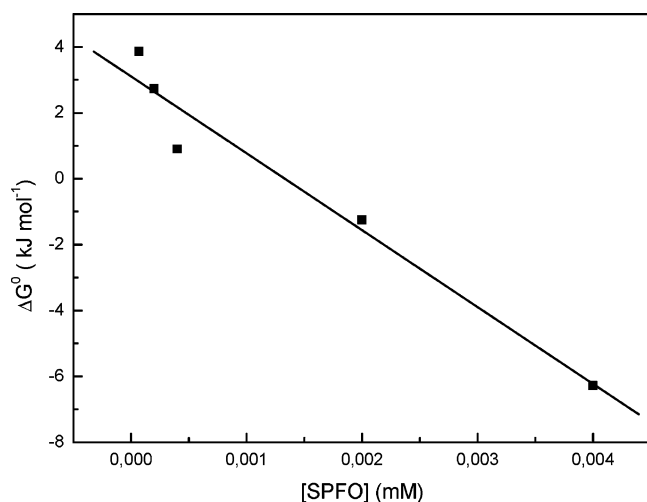


**Figure 5.** Standard Gibbs energy ( $\Delta G^\circ$ ) as a function of surfactant concentration for the IgG conformational transition at 25  $^\circ$ C.

ion sites occurred, and the binding sites for such interactions saturates quickly ( $g_1 = 3$ ). This leads to less strong ( $n_{H_2} = 0.43$ ) but cooperative hydrophobic interactions that favor the union of a big quantity of surfactant molecules ( $g_2 = 1102$ ). This fact

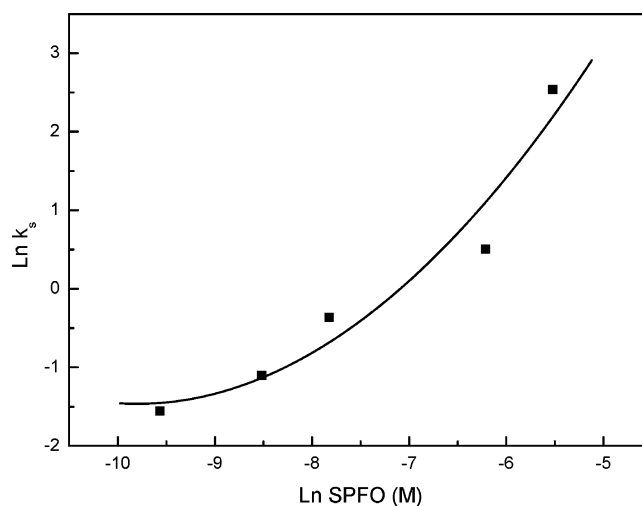


**Figure 6.** Relationship between  $\ln K_s$  and  $\ln[\text{SPFO}]$  at 25  $^\circ$ C.

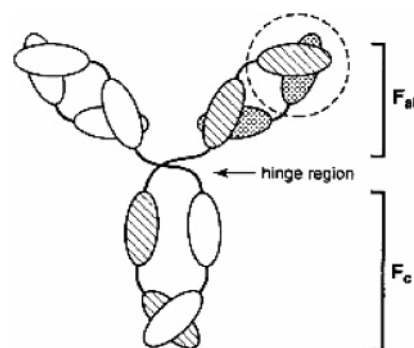


**Figure 7.** Schematic diagram of IgG, showing the  $F_{ab}$  and  $F_c$  fragments and the hinge region.

is explained<sup>13,14</sup> by the presence of the perfluorinated chains in the surfactant molecule. As the most electronegative of all elements, fluorine has very special properties. It has a high ionization potential and very low polarizability. Yet this relatively small atom is significantly larger than hydrogen (van der Waals radius of 1.47  $\text{\AA}$  vs 1.20  $\text{\AA}$ ). Consequently, perfluoroalkyl chains are more bulky than their hydrogenated counterparts (cross section: 30  $\text{\AA}^2$  vs 20  $\text{\AA}^2$ ). The average volumes of the  $\text{CF}_2$  and  $\text{CF}_3$  groups are estimated to be 38  $\text{\AA}^3$  and 92  $\text{\AA}^3$ , respectively, as compared to 27  $\text{\AA}^3$  and 57  $\text{\AA}^3$  for the  $\text{CH}_2$  and  $\text{CH}_3$  groups. Another consequence of the larger size of the fluorine atom is the greater stiffness of perfluorinated chains, which is related to the loss of gauche/trans freedom. The gauche/trans energy difference is ca. 2.0  $\text{kJ mol}^{-1}$  and 4.6  $\text{kJ mol}^{-1}$  for hydrocarbon and hydrocarbon chains, respectively. In order to minimize steric hindrance, perfluorinated chains adopt a helical conformation. Furthermore, the dense electron cloud of the fluorine atom results in a repellent sheath that protects the perfluorinated chain against the approach of reagents. The low polarizability of fluorine results in low van der Waals interactions between fluorinated chains and low cohesive energy densities in liquid fluorocarbons. These low interactions are responsible for many of the most valuable properties of fluorocarbons, such as very low surface tension, excellent spreading properties, high fluidity, and so forth. The large surface presented by the fluorinated chains (the hydrophobic effect of the chain is roughly proportional to its area in contact with water), in conjunction with the low polarizability of the fluorine atoms, results in enhanced hydrophobicity. Perfluorinated chains thus combine two characteristics that are usually considered to be antinomic: they are extremely hydrophobic



and lipophobic at the same time.<sup>15</sup> Thus, surfactant tails interact strongly with lipophobic as well as lipophilic residues in IgG domains.

Employing eq 4, we determine the Hill graph and calculated Hill binding for the SPFO–IgG hydrophobic interaction. It was found that  $k_H = (8.9 \pm 0.4) \times 10^{-2}$ .

An important thermodynamic parameter that characterizes the surfactant–protein binding is the binding Gibbs energy, calculated per surfactant molecule bound per monomeric IgG ( $\Delta G_\nu$ ). To obtain this parameter for the IgG–SPFO interaction, the binding isotherm was fitted to polynomials of the form

$$\nu = a + b(\log[S]) + c(\log[S])^2 + \dots \quad (11)$$

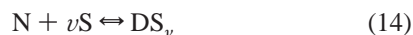
where  $[S]$  is the surfactant concentration. The order of the polynomial was chosen to give the highest correlation coefficient and lowest error over the data point range.

The polynomial was used to calculate the Wyman binding potential ( $\pi$ ) as a function of  $\nu$  from the following equations:<sup>16</sup>

$$\pi = 2.303RT \int_{(\log[S])\nu(=0)}^{(\log[S])\nu} \nu d(\log[S]) \quad (12)$$

$$\pi = 2.303RT \{a(\log[S]) + b(\log[S])^2 + c(\log[S])^3 + \dots\} \quad (13)$$

As a first approximation, the conformational change process can be considered as an interaction between native IgG (N) and surfactant (S) expressed by the following equilibrium:



where  $DS_\nu$  is the formed complex with  $\nu$  surfactant molecules bound. The equilibrium constant ( $K$ ) of eq 14 as a function of  $\nu$  can be calculated by the equation

$$\pi = RT \ln(1 + K[S]^\nu) \quad (15)$$

and hence  $\Delta G_\nu$  as a function of  $\nu$  can be calculated from

$$\Delta G_\nu = -\frac{RT \ln K}{\nu} \quad (16)$$

This procedure leads to a smooth curve of  $\Delta G_\nu$  vs  $\nu$  (Figure 2). The Gibbs energy per molecule bound ( $\Delta G_\nu$ ) moves toward zero when  $\nu$  moves to zero. The plot shows a minimum corresponding to the most tightly bound ligands at low values of  $\nu$ . Then the curve tends to a limiting value of  $-7.41 \text{ kJ mol}^{-1}$ . Similar curves were found in previous works for insulin-*n*-alkylsulfates<sup>17</sup> and for HSA–SPFO interactions.<sup>4</sup>

**3.2. Conformational Changes in IgG Induced by SPFO Binding.** From the potential measurements obtained by the application of an SPFO-selective electrode, it was determined that there were true specific unions between surfactant molecules and IgG structure. The binding of surfactant molecules on IgG domains causes the unfolding of proteins.

To study the effect of SPFO on the IgG conformation, we first establish the IgG adsorption spectra, varying the SPFO concentration. Figure 3 shows the spectra of the native protein and IgG–SPFO mixtures obtained over an SPFO concentration range. The results show an increase in absorbance, reaching a maximum at 280 nm followed by a progressive decline in the magnitude of the absorbance between 290 and 310 nm.

To evaluate the effect of SPFO on the IgG unfolded process, difference spectra for the 280 nm band for native IgG versus SPFO-treated protein were carried out. The results are shown in Figure 4, which illustrates one transition region

in the concentration range of 0.03–6 mM, over which absorbance changes steeply with surfactant concentration. These results suggest that, in the interaction with fluoroamphiphile molecules, the protein undergoes a change in its conformation.

Keeping in mind equilibrium 14, it is assumed that the binding of the surfactant and the conformational changes induced by binding are reversible. The reversibility of the spectral absorbance difference at 280 nm on surfactant dilutions from high to lower concentrations suggests that this is a reasonable assumption. The reaction equilibrium constant ( $K$ ), can thus be written:

$$K = \frac{[DS_\nu]}{[N][S]^\nu} = \frac{K_S}{[S]^\nu} \quad (17)$$

where  $K_S$  is the ratio of surfactant–protein complex and native molecules, and  $[S]$  is the equilibrium concentration of free surfactant. Because in the experiments IgG molarity was very low (0.1  $\mu\text{M}$ ), it is assumed that  $[S]$  is negligibly different from the total surfactant concentration in the system.

Values of  $K_S$  as a function of  $[S]$  for the first and second transition regions were calculated from the absorbance curve ( $A_{280}$ ) in Figure 4 from the extension of denaturation ( $\alpha$ ) taken as

$$\alpha = \frac{A_{280} - A_{280}^N}{A_{280}^D - A_{280}^N} \quad (18)$$

where  $A_{280}^N$  and  $A_{280}^D$  are the absorbances for the native and denaturated states, respectively, and  $K_S = \alpha/(1 - \alpha)$ .  $A_{280}^N$  and  $A_{280}^D$  were taken from the start and finish of the transition region. The pre- $\gamma$ , post-transition curves were fitted by least-squares linear plots, and the transition region was fitted by a polynomial;  $\alpha$  and  $K$  were then calculated by the method described by Pace.<sup>18</sup>

Figure 5 shows the plot of  $\Delta G^0$  as a function of surfactant concentration. The linearity of the plot is consistent with the following relations:

$$\Delta G^0 = \Delta G_W^0 - m[S] \quad (19)$$

$$\ln K_S = \ln K_W - \frac{m}{RT}[S] \quad (20)$$

where  $\Delta G^0$  is the difference in the standard Gibbs energy between the folded and unfolded states.  $\Delta G_W^0$  is the value of  $\Delta G^0$  for the transition in the absence of surfactant,  $m$  is a measure of the dependence of  $\Delta G^0$  on surfactant concentration  $[S]$ , and the  $m[S]$  term thus represents the difference between the unfolded and native states.

The standard Gibbs energy for unfolding in water ( $\Delta G_W^0$ ) can be calculated from  $\ln K_W$  from the intercept of  $\ln K_S$  vs  $[S]$  at  $[S] = 0$ . From eq 17, it follows that

$$\ln K = \ln K_S - \nu \ln[S] \quad (21)$$

Figure 6 shows the plot of  $\ln K_S$  vs  $\ln[S]$ . This plot is not linear as predicted eq 21 but is better represented by the equation

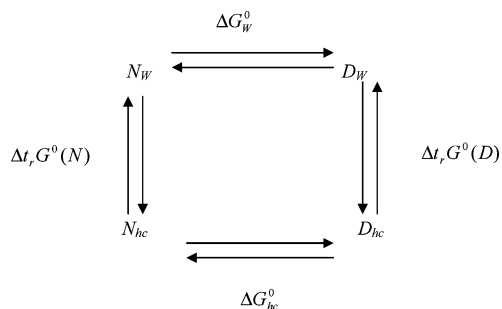
$$\ln K_S = \ln K + \nu \ln[S] + b(\ln[S])^2 \quad (22)$$

The reason for the curvature may be related to the neglect of activity coefficients in eq 17.

**TABLE 1: Parameters Characterizing the Surfactant-Induced Conformational Changes in IgG Aqueous Surfactant Solutions**

SPFO–IgG interaction	$[S]_{1/2}/$ $\text{mmol dm}^{-3}$	$m/$ $\text{kJ mol}^{-1}$	$\Delta G_W^0/$ $\text{kJ mol}^{-1}$	$\nu$	$\Delta G_{hc}^0/$ $\text{kJ mol}^{-1}$	$\Delta(\Delta_t G^0)/$ $\text{kJ mol}^{-1}$
	$0.34 \pm 0.03$	$2335.3 \pm 274.1$	$3.1 \pm 0.5$	$4 \pm 2$	$-43.7 \pm 20.1$	$-46.8 \pm 20.6$

At a surfactant concentration of  $1 \text{ mol dm}^{-3}$ ,  $\ln K = \ln K_s$ , and the equilibrium constant might then be considered to correspond to the transition in a surfactant–saturates complex approximating to that in very hydrophobic environments with a corresponding Gibbs energy change,  $\Delta G_{hc}$ . The determined values of  $\Delta G_{hc}$  and  $\Delta G_W$  can be related by the following Scheme 1:

**SCHEME 1**

where  $N_W$ ,  $N_{hc}$ ,  $D_W$ , and  $D_{hc}$  are the native and denatured protein states in water and hydrocarbon environments, respectively. From Scheme 1 it follows that

$$\Delta G_{hc}^0 - \Delta G_W^0 = \Delta_t G^0(D) - \Delta_t G^0(N) \quad (23)$$

where  $\Delta_t G^0(D)$  and  $\Delta_t G^0(N)$  are the standard Gibbs energies of transfer of denatured and native IgG water to hydrophobic environments, respectively.

Table 1 lists the parameters  $[S]_{1/2}$ ,  $m$ ,  $\Delta G_W^0$ ,  $\nu$ ,  $\Delta G_{hc}^0$ , and  $\Delta(\Delta_t G^0)$  as calculated from eqs 20, 22, and 23 for IgG–SPFO interactions. Similar values of such parameters were obtained in previous works<sup>3,19–22</sup> and for the interaction between SDS and lysozymes.<sup>23</sup> This suggests that the protein suffers a conformational change due to the chemical interaction with SPFO. We can see that conformational changes on IgG structure begin at very low surfactant concentrations. The method did not provide information useful to distinguish between electrostatic and hydrophobic interactions. The higher parameter values detected indicate that the interaction is highly cooperative. This fact was previously inferred from potential data. Therefore, the initial binding of SPFO molecules to the active site could act as a nucleus for further binding and subsequent unfolding.

**3.3. IgG Structural Changes Caused by Chemical and Thermal Unfolding.** Potential and UV–vis spectrophotometric measurements showed that the binding of SPFO onto IgG molecules alters its structure and causes conformational changes in the protein. IgG is best described as a protein containing 12 independent globular domains distributed over four polypeptide chains that are connected by disulfide bonds and noncovalent forces. The four polypeptide chains are grouped together in different fragments—two identical  $F_{ab}$  segments and one  $F_c$  segment—thus forming a Y-shaped structure, (Figure 7).

Figure 8 shows the CD spectra for native IgG and SPFO–IgG solutions. The CD spectra of the pure and mixed IgG are that of a typical immunoglobulin, with a negative band at 217 nm and zero intensity at a wavelength of 206 nm, representing a high content of  $\beta$ -sheets, and several positive and negative bands in the near-UV region (between 260 and 300 nm). There

is a clear decrease in the ellipticity content: the bands become more positive as the SPFO concentration is augmented. A significant fraction of the IgG is denatured, which is reflected by a diminution of the  $\beta$ -sheet content. This fact may be due to the binding of hydrophobic fluorinated tails, which will penetrate into the hydrophobic domains of the globular IgG in order to reduce their contacts with water. Due to such penetration, the IgG molecule may deform as we can observe from the CD–UV spectra.

The surfactant effect is appreciable even at a very low surfactant concentration (0.013 mM). The changes caused by surfactants relative to the folding increase with  $[S]$  in the range of 0.026–0.5 mM; above 0.5 mM, there are no surfactant effects. It was mentioned by Goto et al.<sup>24</sup> that the constant domains of isolated  $F_{ab}$  fragments denature more easily than the variable domains of  $F_c$  fragments. From our study we can infer that, upon increasing SPFO concentration, the  $F_{ab}$  fragments are primarily affected followed by the unfolding of  $F_c$  fragments under even more extreme conditions. The chemical structural changes in protein molecules observed with UV–CD are consistent with the previously obtained potential and with UV–vis spectrometric data.

The CD reference spectra<sup>25</sup> show that, at a wavelength of 206.5 nm, the intensity due to the  $\beta$ -sheet is essentially zero, whereas the other structural elements significantly contribute. Thus, by measuring the ellipticity at 206.5 nm as a function of temperature, one monitors the change in  $\beta$ -turn,  $\alpha$ -helix, and random coil contents. At this wavelength, an increase in  $\beta$ -turns shifts the ellipticity in a positive direction, whereas increased  $\alpha$ -helix and random coil contents cause a negative shift.

The CD temperature scan of native IgG in a water solution at a heating rate of 30 °C/h is given in Figure 9. The ellipticity–temperature profile displays two steps at which intensity strongly decreases, indicating two distinct temperatures where changes in secondary structure occur. These changes correspond with the unfolding of  $F_{ab}$  and  $F_c$  fragments. Similar results were obtained in previous studies.<sup>26–28</sup>

As we know, proteins are comprised of a number of independent, compact, globular regions called domains.<sup>29</sup> Sometimes these domains can be isolated as stable fragments. Interactions between the domains may provide the intraprotein communication that is necessary to coordinate the various protein functions. Goto and Hamaguchi<sup>30</sup> demonstrated that a polypeptide chain segment corresponding to a single domain can be refolded independently of the rest of the protein. However, independent unfolding of different domains is not a general phenomenon. The great majority of proteins show cooperativity in the unfolding transitions due to heat or chemical treatments. An important class of proteins that conform to a common subunit structure are the IgG proteins. These molecules have domains that are structurally independent, with a characteristic fold.<sup>31,32</sup>

Figure 10 shows the thermal ellipticity variation of the IgG–SPFO solutions. It can be seen that the presence of the fluorinated surfactant affects the thermal ellipticity profile. In the presence of the surfactant at the selected concentrations of 0.013, 0.026, and 2 mM, the transitions occur at higher temperature, and the second transition overlaps with the first one. CD data demonstrate that SPFO has a notable effect on

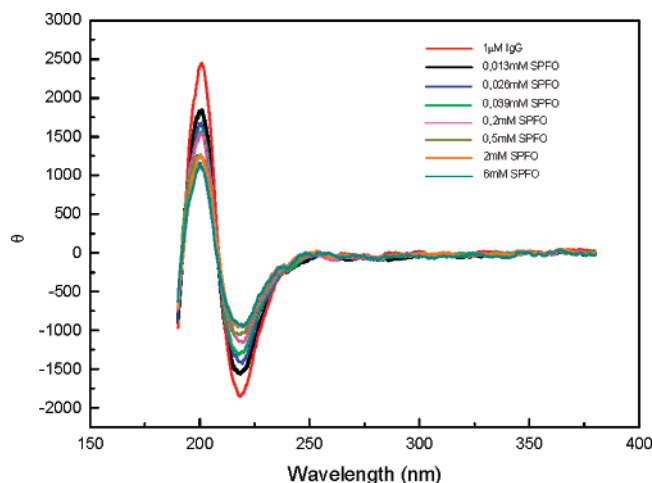


**Figure 8.** UV-CD spectrum of pure IgG and SPFO-IgG mixture solutions. The protein concentration was 1  $\mu$ M.

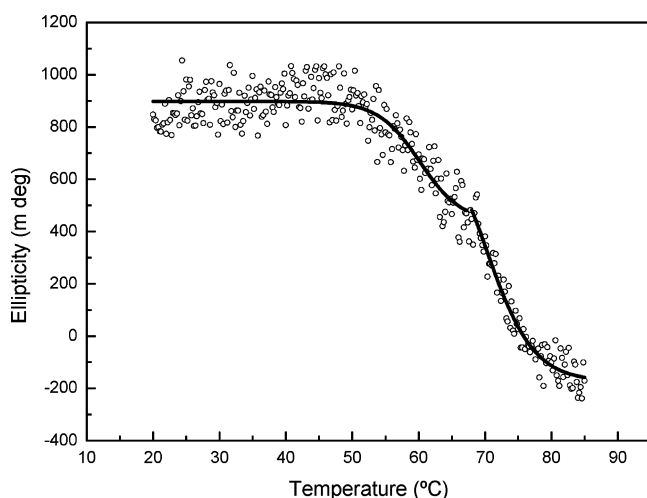


**Figure 9.** UV-CD temperature scan of native IgG in a water solution at a heating rate of 30  $^{\circ}$ C/h.

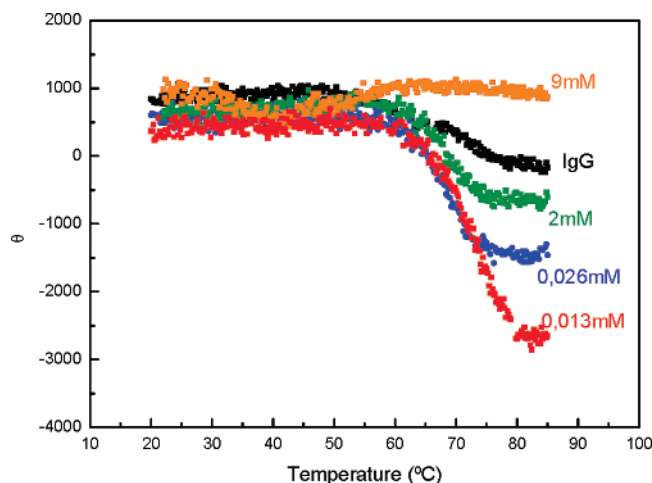


**Figure 10.** Thermal ellipticity variation of the IgG-SPFO mixture solutions at a heating rate of 30  $^{\circ}$ C/h. The protein concentration was 1  $\mu$ M.

the thermal stability of IgG. In the absence of SPFO, the fractions of  $\alpha$ -helix,  $\beta$ -sheet,  $\beta$ -turn, and random coil conformations of native IgG were 0, 66, 22, and 12%, respectively.<sup>29</sup> So, as much for the native IgG as for the surfactant-protein mixtures (0.013–2 mM SPFO concentration) at higher temperatures, the fractions of  $\alpha$ -helix and random coil structures

increase and those of  $\beta$ -sheet and  $\beta$ -turn decrease. For dissolved, native proteins, it is more favorable for the peptide units at the aqueous periphery to form hydrogen bonds with water molecules than among each other. At low surfactant concentration (0.013 mM), part of the hydrophobic interior of the IgG will be exposed to the solution, which, in turn, causes the formation of aggregates. Now, at the interfaces between the building blocks, hydrogen bonds between peptide units in the polypeptide chain may be formed, inducing the formation of  $\alpha$ -helices. Timmins et al.<sup>33</sup> and Zulauf<sup>34</sup> previously showed that the adsorbed amount of surfactant increases with increasing temperature.

Both an increased surfactant concentration as well as the penetrations of hydrophobic IgG domains by hydrophobic perfluorinated tails caused a smaller contribution from intramolecular hydrophobic bonding to the stabilization of globular IgG structure in aqueous solution. As a result, the increment in the percentage of  $\alpha$ -helix decreased. The presence of a high surfactant concentration induces the transference of a significant fraction of the  $\beta$ -sheets into a random coil. The SPFO destabilizing effect can be easily seen from Figure 10; at high surfactant concentration (9 mM), IgG is completely unfolded.

#### 4. Conclusions

From this study, we can conclude that, in the interaction between SPFO and IgG, specific unions are formed. These interactions can be divided in two categories: (1) an initial ionic interaction that saturates all the binding sites and (2) a second cooperative hydrophobic interaction that favors the union of a large quantity of surfactant molecules. The limiting value of the binding Gibbs energy found was of  $-7.41$  kJ mol<sup>-1</sup>. Spectroscopic measurements indicated that IgG allows a conformational transition induce by SPFO. The high thermodynamic parameters found for these conformational changes show a highly cooperative interaction. The ellipticity-temperature profile of native IgG displays two steps at which intensity strongly decreases, indicating two distinct temperatures where changes in the secondary structure occurs. These changes correspond with the unfolding of F<sub>ab</sub> and F<sub>c</sub> IgG fragments.

**Acknowledgment.** The authors acknowledge the financial support from the Spanish “Ministerio de Educación y Ciencia, Plan Nacional de Investigación Científica e Innovación Tecnológica” (I+D+i), Project No. MAT2005-02421, from the “European Regional Development Fund” (ERDF), and from “Xunta de Galicia”, Projects PG1D1T04BTF200014PR and PG1DT06PX1C206048PN. P.M. is an assistant researcher of the “Consejo Nacional de Investigaciones Científicas y Técnicas de la República Argentina (CONICET)”. P.M. thanks the “Fundación Antorchas, Argentina, Project 4308-110” for her grant.

#### References and Notes

- (1) Kissa, E. *Fluorinated Surfactants: Synthesis, Properties, Applications*; Marcel Dekker: New York, 1994.
- (2) Krafft, M. P.; Riess, J. G. *Biochimie* **1988**, *80*, 489.
- (3) Messina, P. V.; Prieto, G.; Ruso, J. M.; Sarmiento, F. *J. Phys. Chem. B* **2005**, *109*, 15566.
- (4) Messina, P. V.; Prieto, G.; Dodero, V.; Ruso, J. M.; Schulz, P.; Sarmiento, F. *Biopolymers* **2005**, *79*, 300.
- (5) Messina, P. V.; Prieto, G.; Dodero, V.; Cabrerizo-Vilchez, M. A.; Maldonado-Valderrama, J.; Ruso, J. M.; Sarmiento, F. *Biopolymers* **2006**, *82*, 262.
- (6) Jones, M. N. *Biological Interfaces*; Elsevier: Amsterdam, 1975.
- (7) Jones, M. N. *Chem. Soc. Rev.* **1992**, *21*, 127.
- (8) Jones, M. N.; Bross, A. *Food Polymers, Gels and Colloids*; Royal Society of Chemistry: Cambridge, U.K., 1991.
- (9) Klotz, I. M.; Hunston, D. L. *J. Biol. Chem.* **1975**, *250*, 3001.



- (10) Scatchard, G. *Ann. N.Y. Acad. Sci.* **1949**, 51, 660.
- (11) Di Cera, E.; Gill, S. J.; Wyman, J. *Proc. Natl. Acad. Sci. U.S.A.* **1988**, 85, 449.
- (12) Hill, A. V. *J. Physiol.* **1910**, 40, 4.
- (13) Bordbar, A. K.; Saboury, A. A.; Housaindokht, M. R.; Moosavi-Movahedi, A. A. *J. Colloid Interface Sci.* **1997**, 192, 415.
- (14) Goddard, E. D. Protein-surfactant interaction. In *Interactions of Surfactants with Polymers and Proteins*; Goddard, E. D., Ananthapadmanabhan, K., Eds.; CRC Press: Boca Raton, FL, 1993; Chapter 4.
- (15) Krafft, M. P. *Adv. Drug Delivery Rev.* **2001**, 47, 209.
- (16) Wyman, J. *J. Mol. Biol.* **1965**, 11, 631.
- (17) Sarmiento, F. G.; Prieto, G.; Jones, M. N. *J. Chem. Soc., Faraday Trans.* **1992**, 88, 1003.
- (18) Pace, C. N. *Tibtech* **1990**, 8, 93.
- (19) Housaindokht, M. R.; Jones, M. N.; Newall, J. F.; Prieto, G.; Sarmiento, F. *J. Chem. Soc., Faraday Trans.* **1993**, 89, 1963.
- (20) Jones, M. N.; Prieto, G.; del Rio, J. M.; Sarmiento, F. *J. Chem. Soc., Faraday Trans.* **1995**, 91, 2805.
- (21) Pombo, C.; Suárez, M. J.; Nogueira, M.; Czarnecki, J.; Ruso, J. M.; Sarmiento, F.; Prieto, G. *Eur. Biophys. J.* **2001**, 30, 242.
- (22) Prieto, G.; Suarez, M. J.; González-Pérez, A.; Ruso, J. M.; Sarmiento, F. *Phys. Chem. Chem. Phys.* **2004**, 6, 816.
- (23) Sun, M. L.; Tilton, R. D. *Colloids Surf., B: Biointerfaces* **2001**, 20, 281.
- (24) Goto, Y.; Ichimura, N.; Hamaguchi, K. *Biochemistry* **1988**, 27, 1670.
- (25) Chang, C. T.; Wu, C. S. C.; Yang, J. T. *Anal. Biochem.* **1978**, 91, 13.
- (26) Vermeer, A. W. P.; Norde, W. *Biophys. J.* **2000**, 78, 394.
- (27) Vermeer, A. W. P.; Norde, W. *Colloids Surf., A: Physicochem. Eng. Aspects* **2000**, 161, 139.
- (28) Vermeer, A. W. P.; Norde, W.; van Amerongen, A. *Biophys. J.* **2000**, 79, 2150.
- (29) Hardie, D. G.; Coggins, J. R. *Multidomain Proteins: Structure and Evolution*; Elsevier: Amsterdam, 1986.
- (30) Goto, Y.; Hamaguchi, K. *J. Mol. Biol.* **1982**, 156, 911.
- (31) Chothia, C.; Novotný, J.; Brucoleri, R.; Karplus, K. *J. Mol. Biol.* **1985**, 186, 651.
- (32) Padlan, E. A. *Mol. Immunol.* **1994**, 31, 169.
- (33) Timmins, P.; Pebay-Peyroula, E.; Welte, W. *Biophys. Chem.* **1994**, 53, 27.
- (34) Zulauf, M. In *Physics of Amphiphiles: Micelles, Vesicles and Microemulsions*; Degiorgio, V., Corti, M., Eds.; Elsevier: Amsterdam, 1985; pp 663-673.